Arthur T. Motta,[1] *Clément Lemaignan,*[1] *and Donald R. Olander*[2]

Segregation of Tin in Zircaloy-2 under Proton Irradiation

REFERENCE: Motta, A. T., Lemaignan, C., and Olander, D. R., **"Segregation of Tin in Zircaloy-2 under Proton Irradiation,"** *Effects of Radiation on Materials: 15th International Symposium, ASTM STP 1125,* R. E. Stoller, A. S. Kumar, and D. S. Gelles, Eds., American Society for Testing and Materials, Philadelphia, 1992, pp. 689–702.

ABSTRACT: Simulating neutron irradiation with charged particles would allow materials to be tested for possible deleterious irradiation effects before being used in reactors. The higher damage rates from charged particle irradiation as compared to neutron irradiation make it possible to achieve comparable doses in significantly smaller times. In this study, tin precipitates between 0.1 and 0.5 μm in diameter were observed at the surface of Zircaloy-2 thin foils after 5.5-MeV proton irradiation. The samples were irradiated to a dose of 1 dpa, at a temperature of 360 K, and a dose rate of 10^{-4} dpa $\cdot$ s^{-1}. X-ray analysis showed the precipitates to be almost pure tin, which was confirmed by diffraction analysis that showed the particles to be β-tin.

A simple model was developed that explains the observations by a preferential solute-interstitial interaction, leading to a defect-induced solute flux to the surface, with consequent precipitation from supersaturated solid solution. The calculation of the solute-interstitial interaction is based on an equilibrium between the two types of interstitials, solute and solvent. The interstitials are created in stoichiometric proportions and then allowed to convert from one type to the other with a difference of δ in the energy barriers for the two conversions. Applying the model to the observations with $\delta = 0.1$ eV yields between two and five monolayers of solute segregated to the surface during the irradiation time.

KEY WORDS: Zircaloy-2, radiation effects, radiation-induced segregation, point-defect properties, charged-particle irradiation

Zircaloy-2 is used throughout the nuclear industry as fuel cladding and structural material inside reactors. Its nominal composition is 1.2 to 1.7% tin, 0.03 to 0.08% nickel, 0.07 to 0.2% iron, and 0.05 to 0.15% chromium in a zirconium matrix [*1*]. While the iron, chromium, and nickel are found in intermetallic precipitates of the types $Zr(Cr,Fe)_2$ and $Zr_2(Ni,Fe)$, tin is in solid solution and has been found to improve the corrosion resistance of Zircaloy [*2*].

Irradiation-induced changes in as-fabricated Zircaloy-2 could vitiate some of its good mechanical properties and corrosion resistance. In particular, the precipitation of the undersaturated tin solid solution could change the corrosion behavior of the material. In that context, charged particle irradiation allows materials to be tested for possible deleterious irradiation effects before their actual in-reactor use. The higher damage rates afforded by charged-particle irradiation in relation to neutron irradiation make it possible to achieve comparable doses in much smaller times, while providing the possibility of temperature and dose rate control.

[1] Research Fellow and Head of Laboratory, respectively, CEA/DRN/SECC, Centre d'Etudes Nucleaires de Grenoble, 85x, 38041 Grenoble CEDEX, France.

[2] Professor, Department of Nuclear Engineering, University of California, Berkeley, and Senior Sci-

In this study we report the results of a 5.5-MeV proton irradiation of Zircaloy-2 in which 0.5 μm beta-tin precipitates were found at the foil surface after 1 dpa. This behavior is explained by a simple model applicable at low temperatures that relates the irradiation-induced point-defect flux to the free surface with the segregation of tin. The coupling of the two fluxes leads to a supersaturation of solute at the surface and to its consequent precipitation from solid solution.

Experimental Methods

Thin foils of Zircaloy-2 in the form of strips rolled to a thickness of 25 μm were obtained from Chicago Development Corp. Disks 1 cm in diameter were mechanically punched from the strips. The samples were then annealed at 873 K for 2 h to recover the original microstructure.

A 10-MeV cyclotron built and operated by CTI (Computer Technology Imaging) was used to irradiate a stack of these disks. The target holder used is shown in Fig. 1*a* and schematically in Fig. 1*b*. The foil assembly consisted of stainless steel disks in which a hexagonal pattern of 2-mm-diameter holes (1) was drilled, with the Zircaloy foils (2) sandwiched in between. At three different locations, thermocouples labeled a, b, and c were inserted into the assembly (3) to monitor the temperature variations. To minimize the temperature rise, the foil assembly was tightly screwed to the back flange to which a copper cylinder with water coils at room temperature was attached (4). In addition, the beam was collimated in a preliminary flange to remove the portion that would hit the stainless steel beam stop in the foil assembly. That fraction of beam energy was removed by another set of cooling coils (5). The irradiation chamber was maintained under a vacuum of 10^{-6} torr to minimize sample oxidation. A carbon foil (6) was put in ahead of the collimator to reduce the beam energy to 5.5 MeV and thus avoid the occurrence of nuclear activation in the samples.

Samples were irradiated for 11 h with 5.5-MeV protons, with a current density of 1.3×10^{14} (ion $\cdot$ cm^{-2} $\cdot$ s^{-1}). The beam was reasonably homogeneous, with a variation of about 15% between the center and side holes in the hexagonal collimator. The temperatures on thermocouples a, b, and c were very stable throughout the experiment. Their averages were 340, 350, and 360 K $\pm$ 5 K.

Thin foils for transmission electron microscopy (TEM) were obtained by cutting irradiated disks with microscissors and thinning with one-sided ion milling. They were then examined on a Jeol 200CX Analytical Microscope at the National Center for Electron Microscopy at the Lawrence Berkeley Laboratory and in a Jeol 1200EX with energy dispersive x-ray (EDX) capabilities at the Centre d'Etudes Nucleaires de Grenoble.

Experimental Results

The conversion from irradiation current to atomic displacements was done using the TRIM-88 code [*3*]. The displacement profile obtained for 5.5-MeV H ions in Zr from TRIM-88 using a displacement energy of 25 eV [*4*] is shown in Fig. 2, where the dose in dpa is plotted against foil thickness for the six foils which the beam transverses. The range is 136 μm, which means that the beam goes through five foils and stops at a depth of 11 μm into the sixth. This theoretical displacement profile was confirmed by postirradiation examination of the samples. The foils showed surface discoloration on the places where the beam had hit the foil through the holes in the collimator (Fig. 1). The discoloration was observed on the front and back of Foils 1 through 5 and on the front of Foil 6. The back of Foil 6 as well as Foils 7 and 8 were examined and found to be unaffected. This observation confirms that the beam was stopped

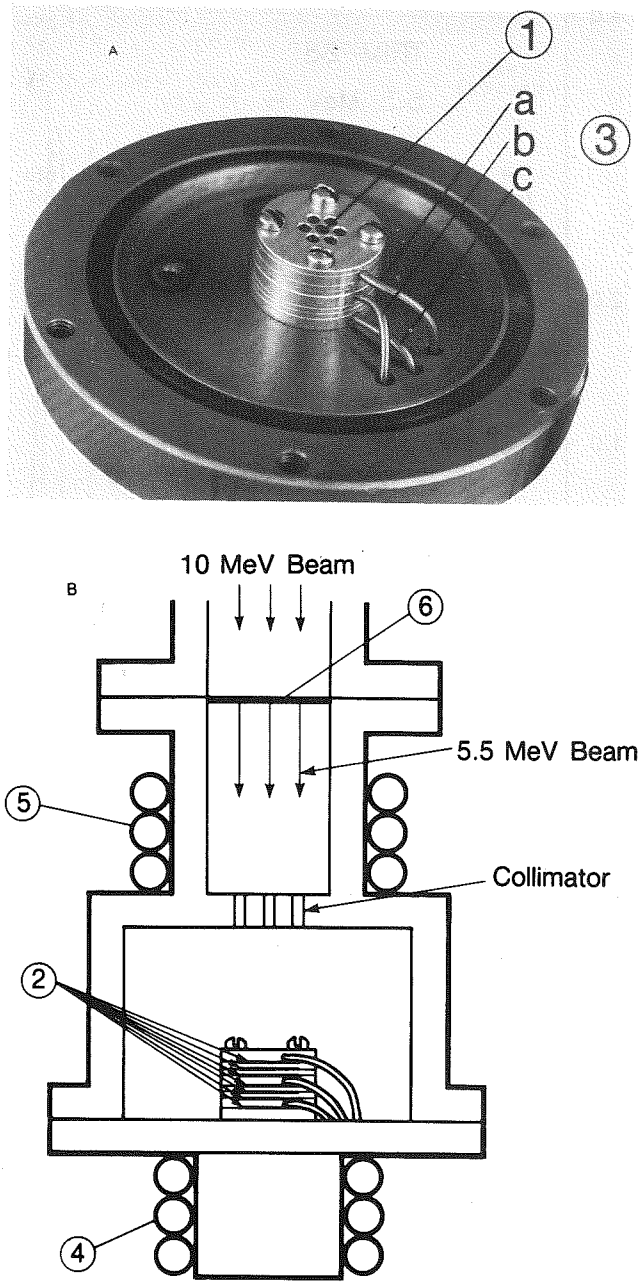

FIG. 1—A, B, *Target Holder Assembly.*

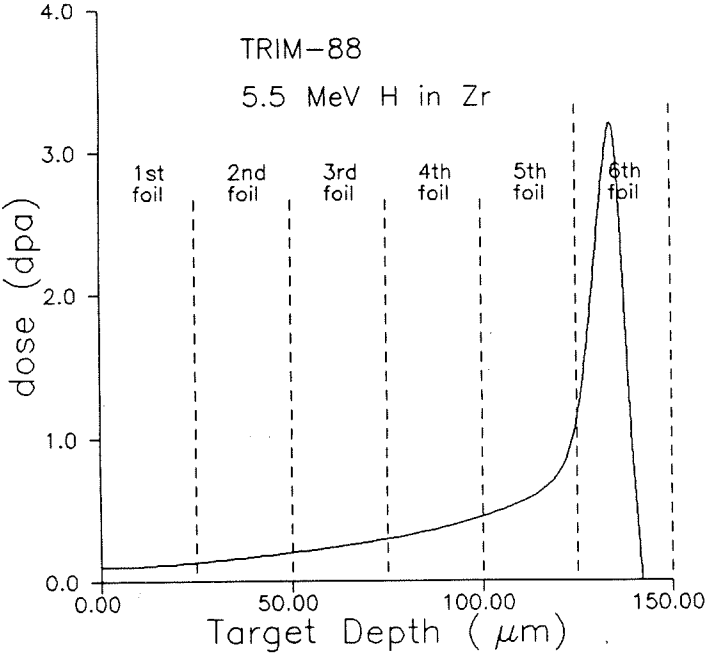

FIG. 2—*Irradiation dose in dpa against penetration distance in microns, as calculated by the TRIM 88 code, for a fluence of* 6×10^{18} *cm*$^{-2}$ *5.5-MeV protons in zirconium, using a displacement energy* $E_d = 25$ *eV.*

The intermetallic precipitates in Foils 1 to 4 were found to be unaffected by the present irradiation, that is, they were crystalline and their number density did not change. In Foils 5 and 6 it was determined that the precipitates are crystalline, but, due to the high degree of damage in the matrix, it was not possible to determine whether their number density had changed.

Segregation of tin was found at the back surface of Foil 5 and at the front surface of Foil 6. Irradiation conditions at that depth were a dose of 1.0 to 1.5 dpa with a dose rate of 4×10^{-5} dpa/s at a temperature between 350 and 360 K.

Most of the segregated tin was found in tin-rich precipitates. These were roundish precipitates with an average diameter of 0.5 μm and no particular orientation relationship with the matrix that could be determined. Since those foils were prepared by ion milling, the tin precipitates could not be polishing artifacts as mentioned in [5]. The EDX spectrum of one of the precipitates from Foil 5, taken with a 20-nm probe, is shown in Fig. 3*a*, and the corresponding tin X-ray map in Fig. 3b. The very large tin concentration in the particle is readily apparent. Quantitative X-ray analysis of the precipitates showed tin concentrations in the precipitates in excess of 90%. Since in the Sn-Zr phase diagram there are no compounds containing more than 66% Sn [*6*], it is likely that the particles in question are pure tin. Most precipitates were too thick for a diffraction pattern to be obtained. On the thin ones, such as the precipitate shown in Fig. 4, diffraction analysis confirms this hypothesis since the patterns obtained can be indexed as the tetragonal β-Sn phase, with lattice parameters $c = 3.18$ A and $a = 5.83$ A [*6*], as shown in Fig. 4.

A line trace of tin content across a tin precipitate/Zr matrix interface was also taken, revealing a constant value of 90% inside the precipitate decreasing quickly to the matrix value at the

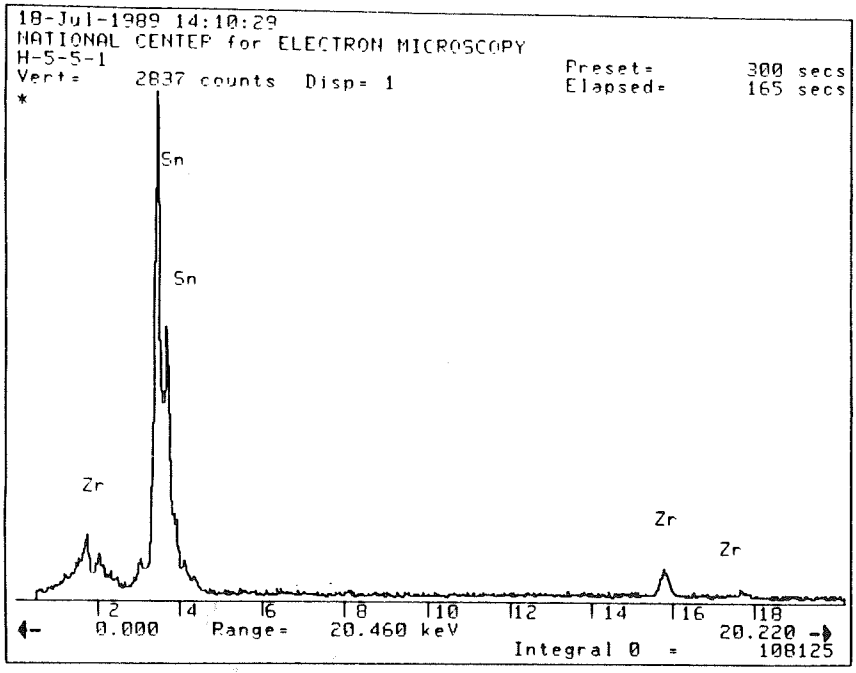

FIG. 3—*(a) EDX spectrum of the tin precipitate in Fig. 3b. The concentration of Sn inside the precipitate is 91 wt%.*

edge. Some depletion in the matrix was also found, the tin content in the matrix near some of the precipitates decreasing from the nominal 1.4% to an average of about 1% in weight.

In two of the seven precipitates examined, a slightly higher concentration of iron was found in the matrix surrounding the precipitates, corroborating the result presented in Ref *7*. Not all segregated tin was found in the tin precipitates. The region between the two precipitates in Fig. 4 is rich in tin (about 16% in weight at Point C). Higher tin concentrations (between 5 and 10%) were also found near $Zr_2(Ni,Fe)$ precipitates but not near $Zr(Cr,Fe)_2$ precipitates.

Theory

Irradiation-induced segregation and precipitation is a well-known phenomenon, both theoretically and experimentally [*8–11*], although it usually occurs at higher temperatures than in the present study.

In the specific case of tin in Zircaloy, Woo et al. [*7*] have reported two types of tin precipitates in neutron-irradiated Zircaloy-2 to a fluence of 3 dpa, at a dose rate of 4×10^{-7} dpa $\cdot$ s^{-1}, and a temperature of 875 K. The authors suggested that the phenomenon may be linked to the irradiation-enhanced diffusion of tin atoms migrating through a substitutional mechanism. They also indicated that iron can help stabilize the tin clusters by annihilating trapped vacancies.

Theoretical treatments of the problem [*8,11*] have found irradiation-induced segregation to derive from a preferential interaction of the solute atoms with either the irradiation-induced vacancy or interstitial defect flux towards the sinks in the material. This interaction can take

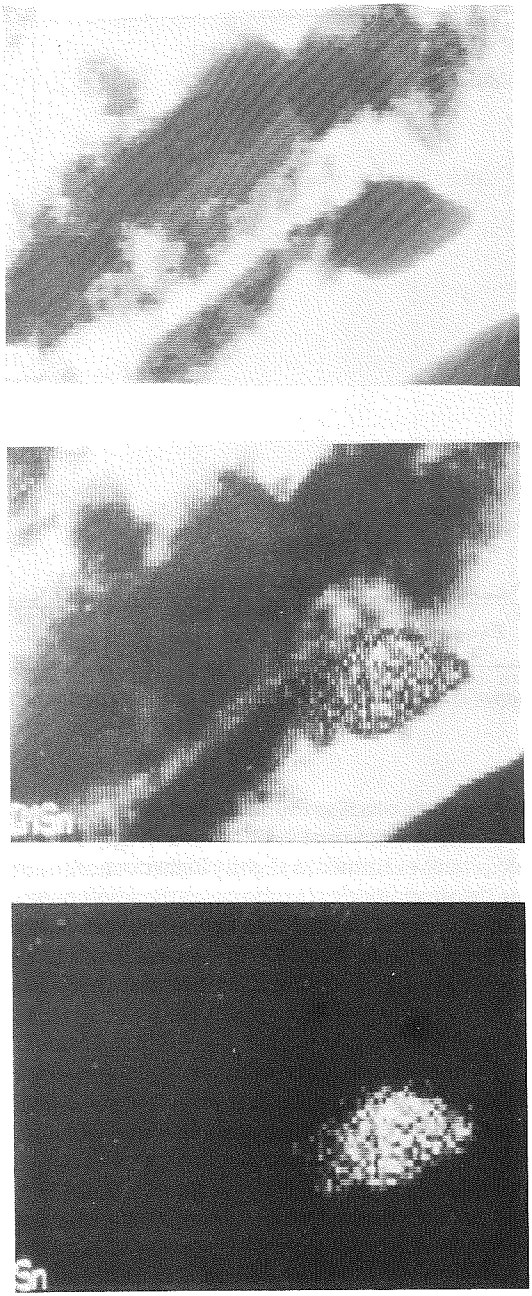

FIG. 3—(b) *X-ray maps corresponding to the EDX spectrum in Fig. 3a. On the upper left is the STEM image of the precipitate. On the upper right and lower left the image is superimposed to the Sn and Zr maps. On the lower right, the Sn map is shown alone.*

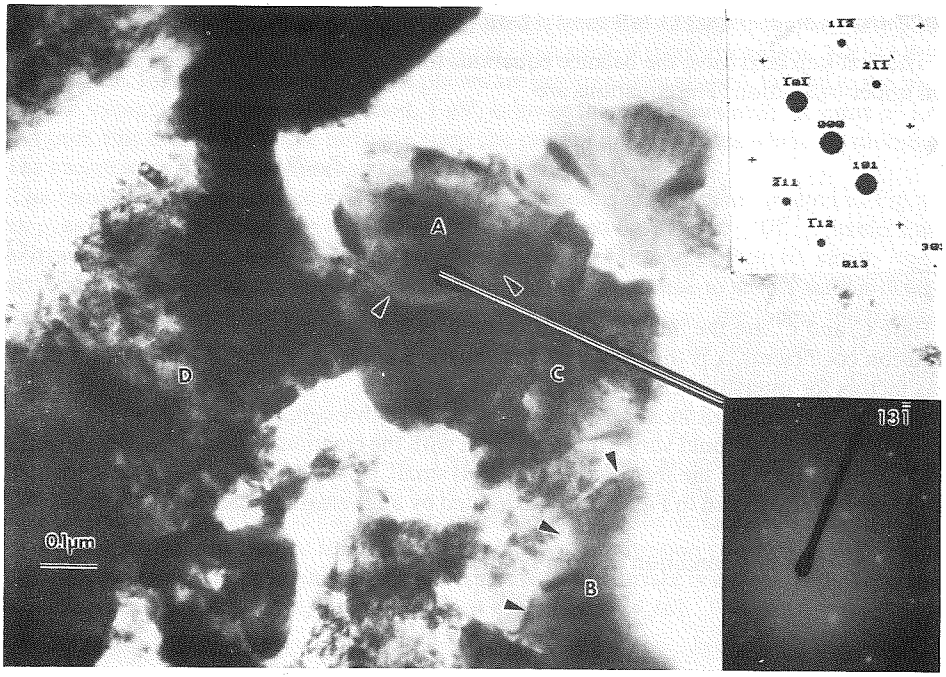

FIG. 4—*Two tin precipitates (A and B, shown by arrows) with tin-rich Region* C *in between. Also shown is a diffraction pattern from Precipitate A, indexed as the 131 zone axis of bct β-tin. The percentage of tin in Precipitates A and B was 93.4 and 92.5%, respectively. The concentration of tin in the zirconium matrix at locations C and D is 16 and 3 wt%, respectively.*

the form of diffusion of mobile solute-defect complexes or of an inverse Kirkendall effect where a defect concentration gradient induces solute segregation. In the first case, the solute is carried along with the defect to the sink so that segregation is observed at the sink. In the second case, vacancies carry the solute away from the sink while interstitials carry the solute towards the sink.

We now present a simple calculation with the objective of demonstrating that the effect observed in this work can be explained by an irradiation-induced segregation mechanism based on interstitial conversion. In previous studies the equations for the point-defect balances are solved, coupled with an equation for the solute concentration, to find the amount segregated at the sink [*8,10,11*]. This is essentially the same as is done in this work, except that we use a simplified approach that allows us to decouple the solute concentration from the point-defect equations by considering the conversion of solvent interstitials to more energetically favored solute interstitials. The point-defect balances are solved in the section below for the conditions appropriate to the experiment, and in the following section, a relationship is derived between the point-defect fluxes and the solute flux.

It should be noted that there is no particular experimental evidence in our work that points to the interstitial as the defect species responsible for solute segregation. However, at low temperatures, for the defect migration energies usually found [*12,13*] ("facile vacancy migration" [*13*] excepted), only interstitials are mobile, so they were assumed in this case to be responsible for the observed solute segregation.

Point-Defect Balances

The first step is to solve the balance equations for the point-defect concentration in a thin foil under irradiation. The equations are

$$\frac{\partial C_i}{\partial t} = D_i \frac{\partial^2 C_i}{\partial x^2} + G - K_{iv} C_i C_v - Z_i \rho_d D_i C_i \tag{1}$$

$$\frac{\partial C_v}{\partial t} = D_v \frac{\partial^2 C_v}{\partial x^2} + G - K_{iv} C_i C_v - Z_v \rho_d D_v C_v \tag{2}$$

Here C_i and C_v are the interstitial and vacancy concentrations, D_i and D_v their respective diffusion coefficients, x is the distance from the foil midplane, Z_i and Z_v are the dislocation bias factors for interstitials and vacancies, and $K_{iv} = K_{iv0} \cdot (D_i + D_v)$ is the recombination coefficient. A constant dislocation density ρ_d is assumed throughout the irradiation. This is an approximation, as ρ_d could vary with irradiation with the creation of new loops, but the influence of dislocations on the segregation process is small, as will be seen. The space-dependent displacement rate shown in Fig. 2 is approximated by an average displacement rate in the foil, G (dpa $\cdot$ s^{-1}).

The first boundary condition is, from symmetry

$$\frac{\partial C_i}{\partial x} = \frac{\partial C_v}{\partial x} = 0 \text{ at } x = 0 \tag{3}$$

The second from considering the surface a perfect sink

$$C_i = C_v = 0 \text{ at } x = L \tag{4}$$

where L is the foil half-thickness. At low temperatures the thermal defect concentration can be neglected, so the initial condition is

$$C_i = C_v = 0 \text{ at } t = 0 \tag{5}$$

Equations 1 through 5 were solved numerically for the parameter values shown in Table 1. For simplicity, no distinction is made here between the migration energies of the two different interstitials. This could be taken into account by writing one point-defect equation for each type of atom. For this approximate treatment, it was decided not to do so. If the migration energy of Sn in Zr is significantly different than that for Zr self-diffusion, then this approximation will need to be reviewed.

TABLE 1—*Parameter values for which Eqs 1 through 5 were solved.*

G = displacement rate = 10^{-4} dpa $\cdot$ s^{-1}
D_i = interstitial diffusion coefficient = $10^{-2} \exp(-0.5\ [\text{eV}]/\text{kT})$ cm^2 $\cdot$ s^{-1}
D_v = vacancy diffusion coefficient = $10^{-2} \exp(-1.0\ [\text{eV}]/\text{kT})$ cm^2 $\cdot$ s^{-1}
K_{iv} = recombination coefficient = 10^{16} [cm^{-2}]$(D_i + D_v)$ s^{-1}
t = irradiation time = 4×10^4 s
L = foil half thickness = 10^{-3} cm
ρ_d = dislocation density = 0 to 10^2 cm^{-2}
Z_i = interstitial dislocation bias factor = 1.2
Z_v = vacancy dislocation bias factor = 1.0

The value for the interstitial migration energy used is from Ref *12* for self-interstitial migration perpendicular to the basal plane in hexagonal close packed (hcp) zirconium. We use this value because, for a rolled sheet, the basal planes are preferentially aligned parallel to the surface. The vacancy migration energy used, 1 eV, is lower than the more realistic value of 1.4 eV. Again, this is a conservative estimate since the present analysis holds when the mobility of the vacancies is much smaller than that of the interstitials.

The results for the interstitial and vacancy concentrations against x are plotted in Fig. 5, with ρ_d as a parameter. For $\rho_d = 0$, a steady state is achieved only for $t > 10^{10}$ s, therefore all the irradiation time consists of the recombination-controlled approach to steady state described in Refs *14* and *15*. For a given vacancy mobility, the time to steady state is determined by the interstitial/vacancy mobility ratio. The bigger the ratio, the longer the time to steady state. Since these results were obtained using a lower bound for that ratio, it is safe to say that steady state is not attained for the irradiation conditions used. This is of only moderate importance to the segregation problem since the controlling factor for solute segregation is the interstitial concentration gradient at the foil surface, which does not vary much (5% at the most) during the approach to steady state. The presence of dislocations tends to lower point-defect concentrations in the bulk but does not change the nature of the solution.

The interstitial concentration curve decreases smoothly into the surface, the gradient at the surface being slightly higher for lower ρ_d. The vacancy concentration curve has a maximum in the foil due to a decrease in the recombination rate as the surface is approached due to the lower interstitial concentration, falling to zero at the surface [*14,16*].

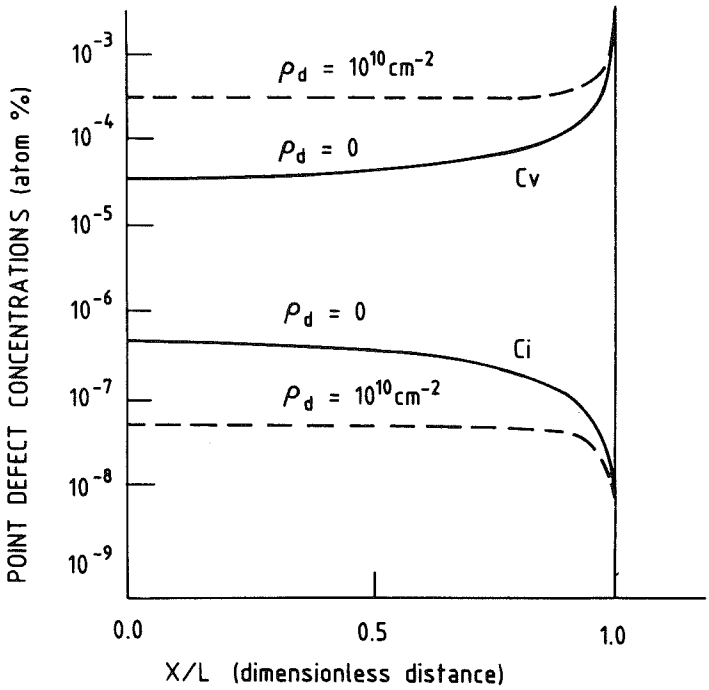

FIG. 5—*Point-defect concentrations against dimensionless distance from the center of the foil, at* t = 4 × 10[illegible] *s, for two values of the dislocation density.*

Equilibrium between Solute and Solvent Interstitials

A relationship is now derived between the point-defect and solute fluxes. The following assumptions are made.

1. Vacancy migration is neglected with respect to interstitial migration, so solute migration occurs only by an interstitial mechanism. This is justified because the vacancy mobility is much lower than the interstitial mobility at low temperature.
2. Interstitial solute atoms have a different formation energy than the corresponding solvent interstitial atoms. Conversion is allowed from one type of interstitial to the other. It is assumed that Sn interstitials have a lower formation energy than Zr interstitials.
3. Since the total segregated percentage of solute atoms is small ($\approx 10^{-6}$), the concentration of tin atoms in the bulk, f, is considered not to vary during irradiation.

Now consider a lattice with C_i interstitials, f atom% tin and $1 - f$ atom% zirconium. Interstitials are created at a rate G (dpa $\cdot$ s^{-1}) in stoichiometric proportions. That is, the displacement energies are taken to be the same for both zirconium and tin. In diffusing through the lattice with, for example, the caging motion proposed in Ref 8, interstitials can exchange places with lattice atoms, thereby allowing the conversion of one type of interstitial to the other. There is therefore an exchange flux of solute (tin) atoms between the lattice and the ensemble of interstitial sites. f^* is defined as the percentage of interstitials that are solute atoms.

The general conversion reaction can be written:

$$\mathrm{Sn}^l + \mathrm{Zr}^i \underset{E+\delta}{\overset{E}{\rightleftharpoons}} \mathrm{Sn}^i + \mathrm{Zr}^l \tag{6}$$

Here Sn^l and Zr^l are tin and zirconium atoms in the lattice and Sn^i and Zr^i are tin and zirconium interstitials. Equation 6 describes an interaction between a tin atom and a zirconium interstitial transforming to a zirconium lattice atom and a tin interstitial. The forward reaction has an energy barrier E and the reverse reaction an energy barrier $E + \delta$. The different barriers lead to an equilibrium between the two lattices in which f^* is different from f.

The solute atom fluxes J_{LI}, from the lattice into the interstitial positions, and its reverse flux J_{IL} from the interstitial positions to the lattice, are:

$$J_{LI} = \nu f(1 - f^*)ZC_i \exp(-E/kT) \tag{7}$$

$$J_{IL} = \nu f^*(1 - f)\, ZC_i \exp[-(E + \delta)/kT] \tag{8}$$

where ν is the vibration frequency (s^{-1}), Z the number of nearest neighbors, T the irradiation temperature, and k the Boltzman constant.

The rate of change in f^* is

$$\frac{df^*}{dt} = J_{LI} - J_{IL} \tag{9}$$

For equilibrium $J_{LI} = J_{IL}$, we obtain

$$(1 - f^*)f = f^*(1 - f) \exp(-\delta/kT) \tag{10}$$

Defining $\alpha = (1 - f)/f$

$$f^* = 1/\{1 + [\alpha \exp(-\delta/kT)]\} \tag{11}$$

In order to have $f^* > f$, δ must be positive. This will happen if the Sn interstitial has a lower formation energy than the Zr interstitial. In that case, the interstitials are formed in stoichiometric proportions, but the Zr interstitials convert to Sn interstitials according to the equilibrium given by Eq 11. Taking the limits $\delta \to 0$ and $\delta \to \infty$, we obtain $f^* = f$ and $f^* = 1$, respectively, as would be expected.

In Fig. 6, f^* is plotted against δ/kT for the value of α normally found in Zircaloy (the percentage of Sn in standard Zircaloy is about 1.2% [*1*], which makes $\alpha = 82$). The exponential in Eq 11 makes the value of f^* rise abruptly with δ/kT, so that even a small difference in formation energy between the two types of interstitials implies a large departure from stoichiometry in f^*. For example, at $T = 350$ K, an energy difference of 0.15 eV makes $f^* = 0.64$.

The net flux of tin atoms to the surface is then

$$J_{Sn} = (f^* - f)\, J_i = (f^* - f) D_i (dC_i/dx)_{x=L} \tag{12}$$

The solute atoms are assumed to arrive at the surface and form monolayers. After enough monolayers have arrived, precipitation from the supersaturated solid solution will occur. Precipitation kinetics shall not be treated in this work. We assume that about three monolayers are enough to cause precipitation.

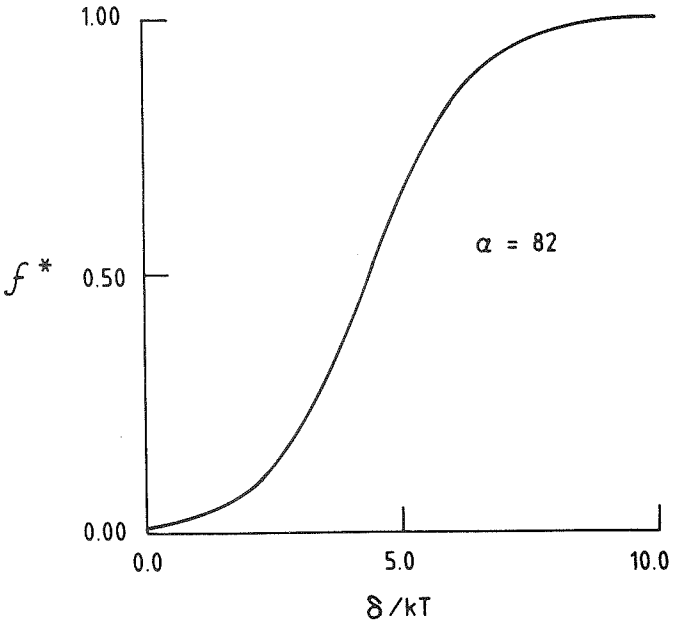

FIG. 6—*Concentration of tin atoms among interstitial atoms,* f*, *against the difference between the solute and solvent interstitial formation energies,* δ, *divided by the thermal energy* kT.

The value of $\delta = 0.1$ eV used in this work is a rough approximation based on a calculation of the change in interstitial elastic interaction energy due to a difference in size between the Zr and Sn atoms, for a Zr/Sn size ratio of 1.011 as given by Pearson and reported in Ref *13*. The elastic interaction energy of the interstitial is proportional to the square of the difference $(r_a - r_s)$ [*17*], where r_a is the atomic radius and r_s is the radius of the preferred site for interstitials in hcp Zr, given by Ref *12*. We then calculate $E_{Sn} \approx E_{Zr} \cdot (r_{Sn} - r_s)^2/(r_{Zr} - r_s)^2 = 3.73$ eV, if $E_{Zr} = 3.83$ eV, which makes $\delta = 0.1$ eV. Taking δ to be that value means taking into account the undersized solute effect and neglecting chemical interactions. Using $\delta = 0.1$ eV in Eq 11 yields a value of 0.25 for f^* at 350 K.

The number, N, of monolayers of solute segregated to the surface per unit area is given by

$$N = \int_0^t J_{Sn}\, dt \tag{13}$$

Figure 7 shows N as a function of irradiation time calculated from Eq 13 for several values of ρ_d. The curves show a practically linear buildup of solute concentration at the surface, reflecting the fact that the gradient at the surface does not vary much during irradiation. The minimum value for precipitation is surpassed at about 5 to 10 h of irradiation.

The influence of a larger dislocation density is to lower the amount of interstitials available to migrate to the surface since some interstitials are absorbed at the dislocations, as mentioned in Ref *8*. However, for the conceivable range of ρ_d values, that is, $0 < \rho_d < 10^{12}$ cm^{-2}, N varies

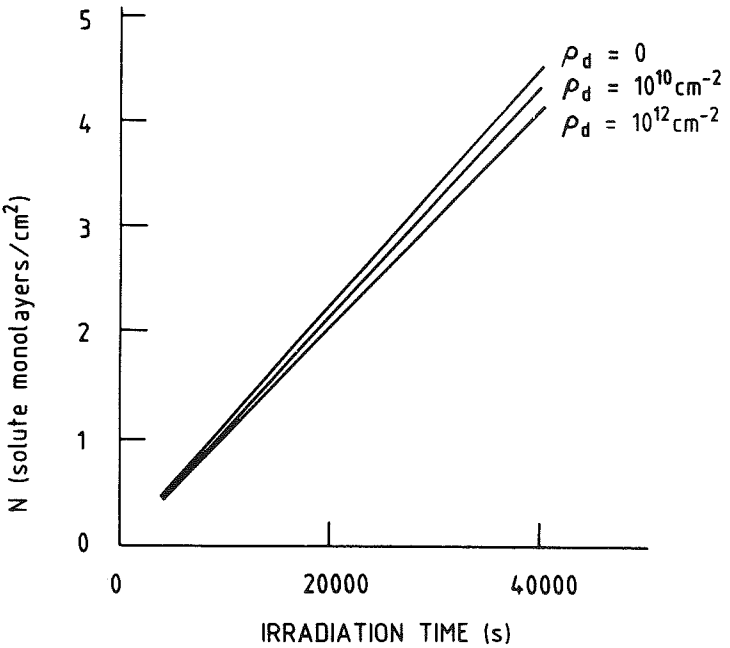

FIG. 7—*Number of tin monolayers segregated to the surface,* N, *as a function of time for* $\delta = 0.1$ *eV, and several values of* ρ_d.

little. This suggests that for the values of ρ_d commonly found (10^8 to 10^{12} cm^{-2}) dislocation density is not an important factor.

Conclusions

1. Precipitates of β-Sn, about 0.5 μm in size were observed at the surface of thin Zircaloy-2 foils after 5.5-MeV proton irradiation at a temperature of 350 K for 4×10^4 s to a dose of 1 dpa.
2. The observation is attributed to irradiation-induced solute segregation to the free surface sink, followed by precipitation from supersaturated solid solution.
3. A model for the segregation kinetics is proposed based on the relative stabilities of solute and solvent interstitials. A configurational energy difference between the two types of interstitials, δ, of 0.1 eV, gives a percentage of solute atoms among interstitials, f^*, of 0.25, which explains the experimental results.
4. No effects on reactor performance should be expected from these experiments, but the interstitial conversion mechanism proposed here could be useful in describing other low-temperature phenomena induced by irradiation.

Acknowledgments

The authors are thankful for the extensive help provided by Computer Technology Imaging of Berkeley, CA, for the irradiations and by the National Center for Electron Microscopy at Lawrence Berkeley Laboratory for X-ray analysis. This work was sponsored in part by the Electric Power Research Institute under Contract Number RP-1250-14 and by the Director, Office of Energy Research, Office of Basic Energy Science, Materials Science Division of the United States Department of Energy, under Contract Number DE-AC03-76SF00098.

One of the authors, Arthur Motta, gratefully acknowledges the support received from CNPq (Brazilian National Research Council) during part of this work.

References

[1] Chemelle, P., Knorr, D. B., Vander Sande, J. B., and Pelloux, R. M., *Journal of Nuclear Materials,* Vol. 113, 1983, pp. 58–64.
[2] Chirigos, J. N., Kass, S., Kirk, W. W., and Salvaggio, G. J., in *Proceedings of the International Atomic Energy Agency, Symposium on Fuel Element Fabrication,* Academic Press, London, 1961, pp. 19–55.
[3] Ziegler, J. F., Biersack, J. P., and Littmark, U., *Stopping and Range of Ions in Solids,* Pergamon Press, New York, 1985.
[4] Griffiths, M., *Journal of Nuclear Materials,* Vol. 165, 1989, pp. 315–317.
[5] Yang, W. J. S., Tucker, R. P., Cheng, B., and Adamson, R. B., *Journal of Nuclear Materials,* Vol. 138, 1986, pp. 185–195.
[6] Abriata, J. P., Boltich, J. C., and Arias, D., *Bulletin of Alloy Phase Diagrams,* Vol. 4, No. 2, 1983, p. 147.
[7] Woo, O. T. and Carpenter, G. J. C., *Journal of Nuclear Materials,* Vol. 159, 1988, pp. 397–404.
[8] Johnson, R. A. and Lam, N. Q., *Physical Review B,* Vol. 13, No. 10, 1976, pp. 4363–4375.
[9] Okamoto, P. R., Rehn, L. E., and Averback, R. S., *Journal of Nuclear Materials,* Vols. 108 and 109, 1982, pp. 319–330.
[10] Wiedersich, H. and Lam, N. Q., in *Phase Transformations Under Irradiation,* F. V. Nolfi, Ed., Applied Science Publishers, London and New York, 1983, pp. 1–46.
[11] Martin, G., *Philosophical Magazine A,* Vol. 38, No. 2, 1978, pp. 131–140.
[12] Fuse, M., *Journal of Nuclear Materials,* Vol. 136, 1985, pp. 250–257.

[13] Hood, G. M., *Journal of Nuclear Materials,* Vol. 159, 1988, pp. 149–175.
[14] Rothman, S. J., Lam, N. Q., Sizmann, R., and Bisswanger, H., *Radiation Effects,* Vol. 20, 1973, pp. 223–227.
[15] Motta, A. T., Olander, D. R., and Machiels, A. J., *Effects of Irradiation on Materials:* 14th International Symposium, *ASTM STP 1046,* pp. 424–437.
[16] Motta, A. T., Ph.D. thesis, "Crystalline-Amorphous Transformation of Precipitates in Zircaloy under Electron Irradiation," University of California, Berkeley, 1988.
[17] Ferro, A., *Journal of Applied Physics,* Vol. 28, 1957, pp. 895–900.